The Journal of Infectious Diseases

MAJOR ARTICLE

A Blunted GPR183/Oxysterol Axis During Dysglycemia Results in Delayed Recruitment of Macrophages to the Lung During *Mycobacterium tuberculosis* Infection

Minh Dao Ngo,[1] Stacey Bartlett,[1] Helle Bielefeldt-Ohmann,[2,3] Cheng Xiang Foo,[1] Roma Sinha,[1] Buddhika Jayakody Arachchige,[4] Sarah Reed,[4] Thomas Mandrup-Poulsen,[5] Mette Marie Rosenkilde,[5] and Katharina Ronacher[1,3]

[1]Translational Research Institute, Mater Research Institute, The University of Queensland, Brisbane, Australia, [2]School of Chemistry and Molecular Biosciences, The University of Queensland, Brisbane, Australia, [3]Australian Infectious Diseases Research Centre – The University of Queensland, Brisbane, Australia, [4]Centre for Clinical Research, The University of Queensland, Brisbane, Australia, [5]Department of Biomedical Sciences, University of Copenhagen, Copenhagen, Denmark

Background. We previously reported that reduced GPR183 expression in blood from tuberculosis (TB) patients with diabetes is associated with more severe TB.

Methods. To further elucidate the role of GPR183 and its oxysterol ligands in the lung, we studied dysglycemic mice infected with *Mycobacterium tuberculosis* (Mtb).

Results. We found upregulation of the oxysterol-producing enzymes CH25H and CYP7B1 and increased concentrations of 25-hydroxycholesterol upon Mtb infection in the lungs of mice. This was associated with increased expression of GPR183 indicative of oxysterol-mediated recruitment of GPR183-expressing immune cells to the lung. CYP7B1 was predominantly expressed by macrophages in TB granulomas. CYP7B1 expression was significantly blunted in lungs from dysglycemic animals, which coincided with delayed macrophage infiltration. GPR183-deficient mice similarly had reduced macrophage recruitment during early infection.

Conclusions. Taken together, we demonstrate a requirement of the GPR183/oxysterol axis for positioning of macrophages to the site of infection and add an explanation to more severe TB in diabetes patients.

Keywords. 25-hydroxycholesterol; diabetes; oxysterols; GPR183; tuberculosis.

Type 2 diabetes (T2D) increases the risk for developing active tuberculosis (TB). Tuberculosis patients with T2D comorbidity are at higher risk of adverse TB treatment outcomes and increased mortality [1]. Several different animal models of diabetes show increased susceptibility to TB [2–8]. We previously reported that dysglycemic *Mycobacterium tuberculosis* (Mtb)-infected mice had more severe TB with a trend towards higher lung bacterial burden, significantly lower pulmonary concentrations of tumor necrosis factor-α and interferon (IFN)-γ during early infection (3 weeks postinfection) accompanied by more severe lung pathology at 8 weeks postinfection compared to normoglycemic control animals [2]. Although various mechanisms likely contribute to an impaired host defense in subjects with hyperglycemia, chronic low-grade inflammation leading to defects in the innate immune responses against Mtb and the subsequent delay in activating adaptive immune responses have been suggested as cellular mechanisms of TB susceptibility [6]. This arises, at least in part, through impaired recognition of Mtb by diabetic alveolar macrophages (AMs) [8].

After infection of AMs with Mtb, the lungs are infiltrated by various cell populations, with neutrophils, interstitial monocytes, macrophages, dendritic cells [9], and eosinophils [10] being recruited to the lung during the first 2 weeks of infection. This cellular migration requires effective chemotactic signals to direct the immune cells to the lung, and signals from Mtb-infected AMs are likely to play a critical part [9].

In addition to classic chemokines, oxidized cholesterols, so-called oxysterols, have been identified as chemoattractants controlling the movement of distinct immune cells to position them to specific tissues [11]. The oxysterol 7α,25-OHC, the most potent endogenous agonist for the G protein-coupled receptor GPR183, is produced from cholesterol via 2 hydroxylation steps by the enzymes Cholesterol 25-hydroxylase (CH25H) and Cytochrome P450 Family Subfamily B Member 1 (CYP7B1), respectively. This oxysterol can subsequently be metabolised by hydroxyl D-5-steroid dehydrogenase, 3b- and steroid D-isomerase 7 (HSD3B7) into 4-cholesten-7α,25-ol-3-one

Received 6 January 2022; editorial decision 14 March 2022; accepted 29 March 2022; published online 18 March 2022.

Presented in part: Keystone eSymposia Tuberculosis: Science Aimed at Ending the Epidemic. December 2–4, 2020, Online conference; Lorne Infection and Immunity Conference, February 16–18, 2022, Lorne, Australia.

Correspondence: Katharina Ronacher MSc, PhD. Translational Research Institute, Mater Research Institute, The University of Queensland, Brisbane, QLD 4102, Australia (katharina.ronacher@mater.uq.edu.au).

The Journal of Infectious Diseases® 2022;225:2219–28

https://doi.org/10.1093/infdis/jiac102

[12]. In addition to B cells and T cells, GPR183 is also expressed on innate immune cells such as macrophages and natural killer cells [13, 14]. GPR183 and 7α,25-OHC are important for chemotactic distribution of immune cells to secondary lymphoid organs [15–21] and positioning of innate lymphoid cells (ILCs) in the gut [22, 23].

However, only a few studies evaluated the role of oxysterols in the lung. Various oxysterols were increased in bronchoalveolar lavage fluid from asthma patients and associated with infiltration of eosinophils, neutrophils, and lymphocytes to the lung [24]. The upregulation of CH25H and CYP7B1 was also observed in the inflamed lungs of patients with chronic obstructive pulmonary disease [25]. In a murine model of lipopolysaccharide (LPS)-induced acute lung inflammation, 25-hydroxycholesterol (25-OHC) was upregulated in the lung [26]. However, the role of oxysterols and GPR183 in infectious respiratory diseases including TB has not been investigated. We previously observed significantly lower GPR183 expression in blood from TB patients with T2D compared with TB patients without comorbidities, and lower GPR183 expression correlated with increased TB disease severity assessed by chest x-ray irrespective of diabetes status [27], suggesting GPR183 and 7α,25-OHC may be important in TB pathogenesis.

In the present study, we investigated the role of GPR183 and 7α,25-OHC in immune cell recruitment to the Mtb-infected lung in normoglycemic and dysglycemic mice. We report that CH25H and CYP7B1 are upregulated and 25-hydroxycholesterol concentrations are increased in the lung in response to Mtb infection in normoglycemic mice. In dysglycemic mice, however, the Mtb-infection induced induction of CYP7B1 expression was absent and associated with reduced macrophage infiltration into the lung. Likewise, mice genetically deficient for GPR183, who have higher Mtb loads during early infection [27], had reduced macrophage recruitment upon Mtb infection, which suggests a requirement of GPR183 for effective macrophage infiltration into the lung and effective containment of Mtb.

METHODS

Murine Models and *Mycobacterium tuberculosis* Infection

We have previously characterized the high-fat diet (HFD) murine model of dysglycemia and tuberculosis [2]. In brief, 6-week-old male C57BL/6 mice were fed a HFD, which contained 43% available energy as fat (total fat: 23.50%; SF04-001; Specialty Feeds, Glen Forrest, Western Australia). Control animals were fed normal chow diet (NCD) with 12% available energy from fat for the same period (total fat: 4.60%; Standard rodent diet; Specialty Feeds). At 12 weeks on the respective diets, mice were infected via aerosol using the GlasCol inhalation exposure system (Model A4224; GlasCol LLC, Terre Haute, Indiana, USA) with approximately 150 colony-forming units of Mtb $H_{37}R_v$ as previously described [2]. GPR183KO mice were infected with Mtb as previously described [27]. Tissues were collected for downstream analysis at either 2, 3, 5, or 8 weeks postinfection as indicated in figure legends.

Ribonucleic Acid Extraction and Quantitative Reverse-Transcription Polymerase Chain Reaction

Ribonucleic acid (RNA) was isolated from lung and blood using Isolate II RNA Mini Kit protocol (Bioline Reagents Ltd., London, UK) with slight modification. In brief, blood cell pellet and lung lobes were homogenized in TRIzol, vigorously mixed with chloroform (2.5:1), and centrifuged at 12 000 ×*g* for 15 minutes at 4°C. The RNA in the aqueous phase was precipitated by mixing in 4°C 70% ethanol (1:2.5) followed by column-based RNA isolation using kit protocol including DNase treatment to remove genomic deoxyribonucleic acid (DNA) contamination. Complementary DNA was synthesized using 2 µg of RNA and the Tetro cDNA synthesis kit (Bioline Reagents Ltd.) according to manufacturer's instructions. Gene expression analysis was performed by quantitative real-time polymerase chain reaction (PCR) with SensiFAST SYBR Lo-ROX Kit (Bioline Reagents Ltd.) run on the QuantStudio 7 Flex Real-Time PCR System (Applied Biosystems). All gene expression levels were normalized to Hprt1 internal controls in each sample, and the fold changes were calculated using the $2^{-\Delta\Delta CT}$ method. The list of primers used is given in Supplemental Table S1. Primer efficiencies are provided in Supplemental Figure 2, and consistent amplification of the housekeeping gene Hprt across the experimental conditions is shown in Supplemental Figure 3.

Immunohistochemistry

Formalin-fixed paraffin-embedded lung sections were dewaxed in xylene before hydrating with decreasing ethanol changes. Endogenous peroxidase activity was blocked with 3% hydrogen peroxide (HL001-2.5L-P; Chem Supply, Adelaide, South Australia) for 10 minutes, and antigen was retrieved using proteinase K (P6556; Sigma-Aldrich) in Tris-EDTA pH8 buffer for 4 minutes at room temperature. Nonspecific antibody binding was blocked using Background Sniper (Biocare Medical, Concord, CA). Immunolabeling was performed with rabbit antibodies against IBA1 (019-19741; NovaChem), CYP7B1 (BS-5052R; Bioss Antibodies Inc, Massachusetts, USA), or isotype control (rabbit IgG; 31235; Thermo Fisher) diluted in Da Vinci Green Diluent (Biocare Medical) for 120 minutes. Sections were subsequently incubated with horseradish peroxidase-conjugated goat antirabbit (ab6721; Abcam). To develop reactions, diaminobenzidine (Dako, Agilent) was used as per the manufacturer's instructions for 2 minutes. Sections were counterstained with Mayer's hematoxylin (Sigma-Aldrich), imaged using VS120 slide scanner (Olympus, Tokyo, Japan), and analyzed using Visiopharm software (Visiopharm, Hoersholm, Denmark) or a Olympus BX50 microscope via Olympus

CellSens standard software 7.1 (Olympus). The method of quantification of the positive staining is described in the Supplement and presented as percentage positive stain of total lung section area.

Mass Spectrometric Quantitation of 25-Hydroxycholesterol (OHC) and 7α,25-OHC in Lung Homogenates

The oxysterol quantification method was adapted from McDonald et al [28] and is described in the Supplement.

Ethics Statement

All experiments were carried out in accordance with protocols approved by the Health Sciences Animal Ethics Committee of The University of Queensland (MRI-UQ/413/17 and MRI-UQ/596/18) and performed in accordance with the Australian Code of Practice for the Care and Use of Animals for Scientific Purposes.

RESULTS

Mycobacterium tuberculosis Infection Increases CH25H and CYP7B1 Expression in the Lung Which Results in Increased Oxysterol Production

To investigate whether Mtb-infection induces the production of oxidized cholesterols in the lung, we infected mice with Mtb and determined the messenger RNA (mRNA) expression of oxysterol-producing enzymes. Cholesterol is hydroxylated by the enzyme CH25H to form 25-OHC and subsequently hydroxylated by CYP7B1 to form 7α,25-OHC (Figure 1A), the high-affinity agonist for GPR183. The 7α,25-OHC can be further metabolized by the enzyme HSD3B7. We found that Mtb infection significantly upregulated the expression of both *Ch25h* and *Cyp7b1*, whereas *Hsd3b7* was downregulated in the lung at 3 weeks after infection (Figure 1B, black bars). To determine whether increased expression of these enzymes results in increased oxysterol production, we performed mass spectrometry

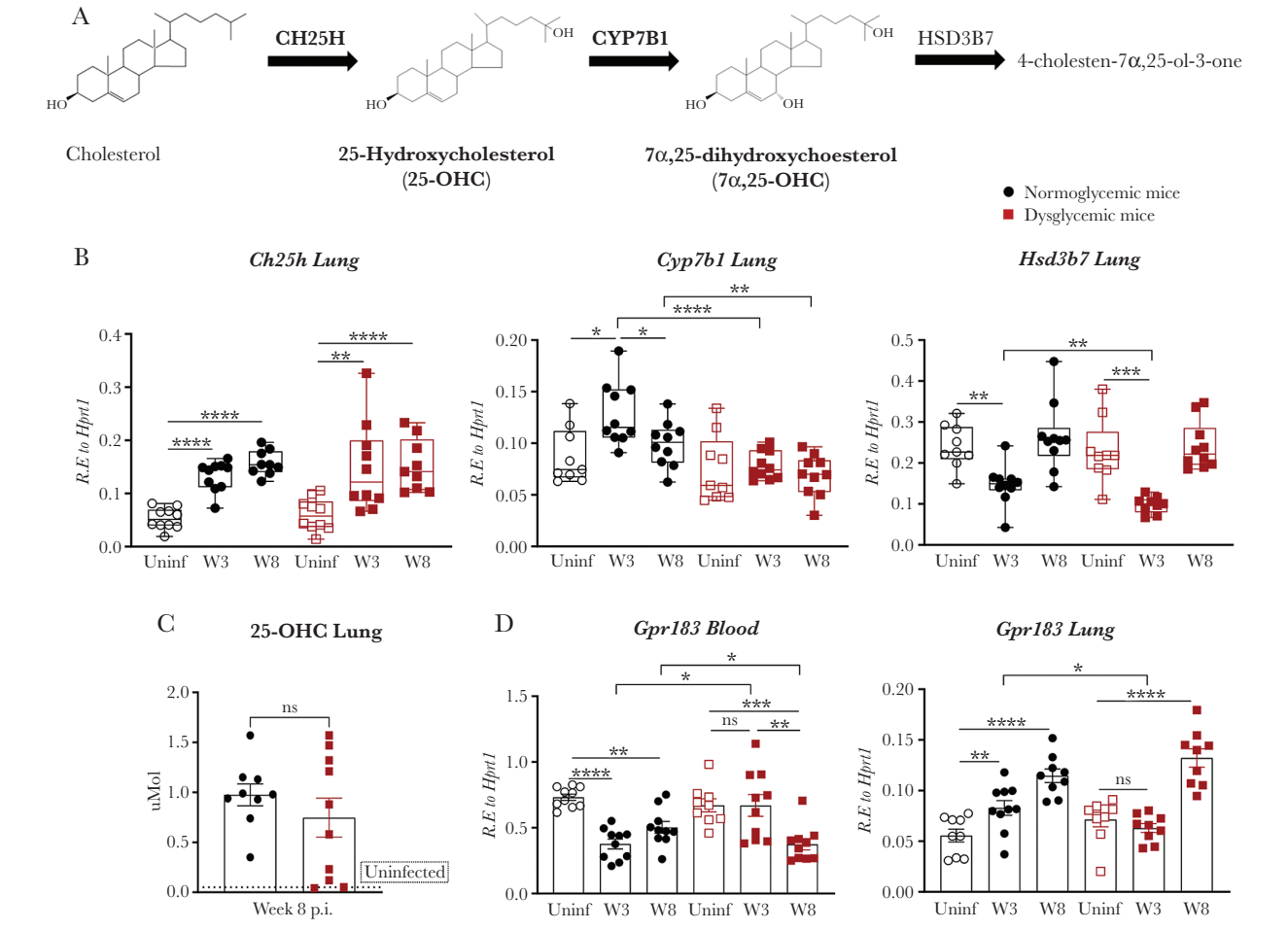

Figure 1. Expression of Ch25h, Cyp7b1, Gpr183, and 25-OHC concentrations in lungs from uninfected (Uninf) and *Mycobacterium tuberculosis* (Mtb)-infected normoglycemic and dysglycemic mice. (A) The biosynthetic pathway of 25-OHC and 7α,25-OHC. Normoglycemic and dysglycemic mice were infected with ~100 colony-forming units aerosolized Mtb $H_{37}R_v$, and mRNA expression of (B) Ch25h, Cyp7b1, and Hsd3b7 was measured by quantitative real-time polymerase chain reaction (qRT-PCR) at 3 and 8 weeks postinfection. (C) Concentrations of 25-OHC were measured in the lungs 8 weeks postinfection. Uninfected mice fed a high-fat diet or normal chow diet are represented by the dotted line. Expression of (D) blood and lung Gpr183 mRNA at 3 and 8 weeks postinfection was determined by qRT-PCR. Data are means ± standard error of the mean of n = 9–10 infected mice/group analyzed from 1 experiment. Circles represent normoglycemic mice and squares represent dysglycemic mice. Data analysis was performed by Mann-Whitney *U* test. *, $P < .05$; **, $P < .01$; ***; $P < .001$; ****, $P < .0001$. ns, not significant.

on lung homogenates for detection of 25-OHC and 7α,25-OHC. The Mtb infection significantly increased 25-OHC production compared to 25-OHC concentrations in uninfected lung homogenates (Figure 1C, black bar vs dotted line). We were unable to accurately determine 7α,25-OHC concentrations in the lung homogenates because they were below the detection limit of the system. However, these results demonstrate that Mtb infection induces expression of *Ch25h* and *Cyp7b1* likely via interferons [29] and results in increased production of 25-OHC and likely also increased production of 7α,25-OHC, both being ligands for GPR183.

Oxysterol Production Is Associated With Increased GPR183 Expression

We have previously reported that lower *GPR183* expression in blood from TB patients is associated with increased TB disease severity on chest x-ray [27] and hypothesized that this is due to chemoattraction of GPR183-expressing immune cells towards a gradient of 25-OHC and 7α,25-OHC to the site of disease, the lung. Consistent with our observation in humans, we found that in Mtb-infected mice *Gpr183* expression decreased in blood compared to uninfected animals, whereas *Gpr183* expression in lung significantly increased upon Mtb infection at both week 3 and 8 postinfection (Figure 1D, black bars). GPR183 expression positively correlated with the expression of the macrophage marker *Adgre1/F4/80* (Supplemental Figure 1). These data suggest that oxysterol sensing GPR183-expressing immune cells migrate towards the lung upon infection.

Dysglycemia Blunts *Mycobacterium tuberculosis*-Induced Expression of CYP7B1 and GPR183 in the Lung

Because diabetes is a well known risk factor for TB and we previously showed that mice with HFD-induced dysglycemia have more severe TB [2], we next investigated whether this is linked to changes in oxysterol production in the lung. We observed that Mtb infection in dysglycemic animals induced *Ch25h* expression similar to normoglycemic animals (Figure 1B, red vs black bars), and the concentrations of 25-OHC were similarly comparable between the animals (Figure 1C, red vs black bar). However, it is interesting to note that the expression of *Cyp7b1* was significantly blunted by dysglycemia and was consistently lower in dysglycemic compared to normoglycemic mice both at week 3 and week 8 postinfection (Figure 1B, red vs black bars). This suggests that the production of 7α,25-OHC is impaired during dysglycemia likely due to insulin resistance [30]. Consistent with this, in dysglycemic animals we did not observe a rapid decrease of *Gpr183* in blood or a rapid increase of *Gpr183* in lung (Figure 1D) within the first 3 weeks postinfection such as observed in normoglycemic animals. *Gpr183* increased only at week 8 postinfection in the lungs of HFD-fed animals.

Taken together, these results demonstrate that Mtb infection results in the production of oxysterols that facilitate the rapid migration of GPR183-expressing immune cells from the periphery to the lung. This GPR183-oxysterol axis is blunted during dysglycemia resulting in delayed recruitment of immune cells to the Mtb-infected lung.

Dysglycemia Blunts CYP7B1 Protein in the Lung After *Mycobacterium tuberculosis* Infection

To further confirm whether the reduced mRNA expression of *Cyp7b1* in dysglycemic animals translates into lower protein expression of CYP7B1, we performed immunohistochemical staining of mouse lung sections with a CYP7B1-specific antibody. We observed that positive signals of CYP7B1 started to accumulate around blood vessels and bronchioles by 3 weeks postinfection with intense signals of CYP7B1 found mostly located in the center of granulomas by week 8 postinfection (Figure 2A). Quantification of positive immunolabeling confirmed the upregulation of CYP7B1 in the lung postinfection (Figure 2B), and the percentage area of CYP7B1(+) was significantly reduced in dysglycemic mice compared to normoglycemic controls at 8 week postinfection (Figure 2B). These results suggest that distinct cell populations involved in granuloma formation drive CYP7B1 expression.

CYP7B1 Is Expressed by Alveolar Macrophages and Infiltrating Macrophages Upon *Mycobacterium tuberculosis* Infection

We next investigate which cell type in the lung produces CYP7B1 upon Mtb infection and found that CYP7B1 was most abundant in alveolar macrophages, identified as large round cells with unsegmented nuclei inside alveolar spaces, of Mtb infected but not in uninfected animals (Figure 3A, middle low image). At week 8 postinfection, intense signals of CYP7B1 were found in the center of granulomas (Figure 3A, right low image). We confirmed that CYP7B1 expression was macrophage derived by immunolabeling lung sections with the macrophage-specific marker ionized calcium binding adaptor molecule 1 (IBA1), the distribution of which overlapped with CYP7B1 expression (Figure 3B). Cells positive for the IBA1 signal started to appear around blood vessels and bronchioles by week 3 postinfection, indicating that $IBA1^+$ macrophages from circulation infiltrated into the lung after Mtb infection, and these $IBA1^+$ macrophages expressed CYP7B1.

Taken together, we demonstrate that CYP7B1 is upregulated in both resident alveolar macrophages and infiltrating macrophages upon Mtb infection and is highly expressed in the center of granulomas. It is thus possible that the oxysterol/GPR183 axis plays an important role in positioning of leukocytes around Mtb-infected macrophages in the TB granuloma.

Dysglycemia Leads to Lower Macrophage Infiltration to the *Mycobacterium tuberculosis*-Infected Lung

We next assessed whether dysglycemia impacts macrophage migration into the Mtb-infected lung. We found that there was more than a 5-fold increase in macrophages within the first 3

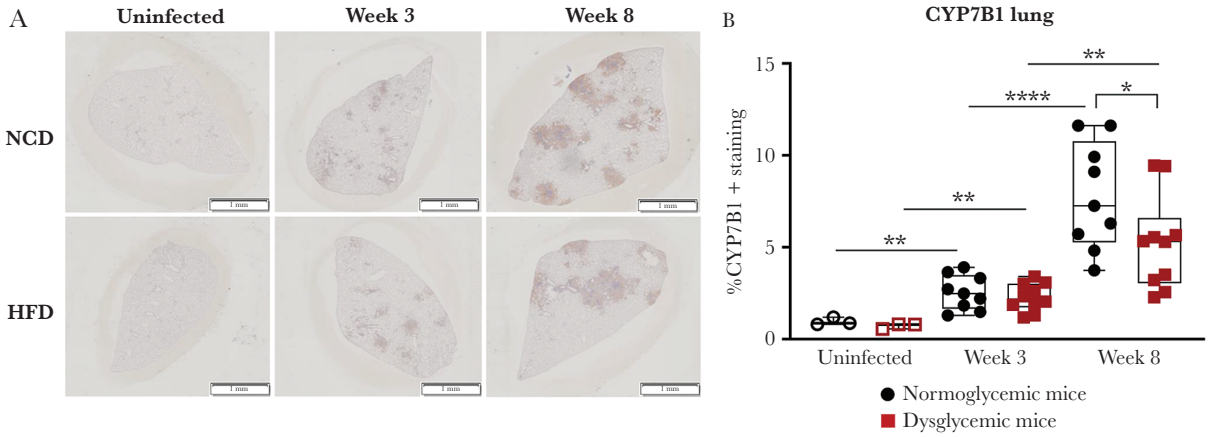

Figure 2. Mice with dysglycemia have lower CYP7B1 at protein levels compared to normoglycemic mice. (A) Representative images of immunohistochemical labeling of CYP7B1 in lung sections from dysglycemic versus normoglycemic mice either uninfected or 3 weeks and 8 week after *Mycobacterium tuberculosis* (Mtb) infection. (B) Quantitative analysis of CYP7B1-immunolabeled areas as percentage of total lung section area. Data are means ± standard error of the mean of n = 9–10 infected mice/group analyzed from 1 experiment. Circles represent normoglycemic mice and squares represent dysglycemic mice. Data analysis was performed by Mann-Whitney *U* test. *, $P < .05$; **, $P < .01$; ****, $P < .0001$. HFD, high-fat diet; NCD, normal chow diet.

weeks postinfection in normoglycemic animals; however, macrophage recruitment was significantly lower in dysglycemic mice at that time point (Figure 4A and B). Taken together, these results suggest that the lower *Gpr183* expression we observed in dysglycemic animals is due to a reduction in macrophage infiltration to the lung during early Mtb infection. We next postulated that the impaired migration of macrophages to the Mtb infected lung is oxysterol/GPR183 dependent.

GPR183 Is Required for Efficient Macrophage Infiltration to the Lung During Early *Mycobacterium tuberculosis* Infection

To investigate whether the GPR183/7α,25-OHC axis is required for macrophage infiltration into the Mtb infected lung, we performed experiments in GPR183KO mice. We previously reported that GPR183KO mice presented with increased Mtb burden compared with wild-type (WT) animals at 2 weeks after infection with Mtb $H_{37}R_v$, an effect that disappeared at 5 weeks postinfection [27]. This suggests that GPR183 plays an important role during the early innate immune response to Mtb infection. We speculated that absence of GPR183 could alter the recruitment and distribution of immune cells to the lung in the context of TB disease. We found that pulmonary macrophage infiltration was significantly reduced in GPR183KO compared with WT mice at 2 weeks postinfection. However, the absence of GPR183 does not result in prolonged macrophage deficiency in the lungs in infected mice. By week 5 postinfection, significantly more macrophages infiltrate the lungs of GPR183KO mice versus WT mice (Figure 5), indicative of a compensatory GPR183/7α,25-OHC-independent mechanism of macrophage recruitment to the lung at that later time point during infection.

These results indicate that GPR183 is necessary for effective recruitment of inflammatory and antimicrobial macrophages to the lung during the early Mtb infection. This early impairment of macrophage migration to the lung likely contributed to higher lung bacterial numbers in GPR183KO mice [27] with a trend towards higher bacterial numbers ($P = .07$) in dysglycemic mice [2].

DISCUSSION

In this study, we demonstrated a role for oxysterols and GPR183 in positioning of immune cells to the Mtb-infected lung with potential implications for other bacterial and viral respiratory tract infections. Previous studies have illustrated the importance of GPR183 in migration of immune cells to secondary lymphoid organs including the positioning of B cells in lymphoid tissues [16, 17], dendritic cells to the marginal zone bridging channels in the spleen [16, 31], T cells in the T cell zone, or, more recently, the localization of ILC3 to lymphoid structures in the colon [22, 32]. However, the role of oxysterols and GPR183 in positioning of immune cells in the lung is largely unexplored. Jia et al [25] showed in a mouse model of COPD that GPR183 is required for the formation of inducible bronchus-associated lymphoid tissue (iBALT), a secondary lymphoid-like structure within the lung. The iBALTs are also formed during Mtb infection and correlate with protection [33]. The initial host determinants that govern the induction of iBALT formation during Mtb infection remain to be elucidated, but it is possible that oxysterols and GPR183 play a major role in iBALT formation during TB by serving as recruitment and retention signals. Our observation that GPR183KO mice are more susceptible to Mtb infection during the first 2 weeks could at least in part be due to deficiencies in iBALT formation. However, it is also possible that the increased Mtb burden is linked to the lower macrophage infiltration we observed during early infection in GPR183KO

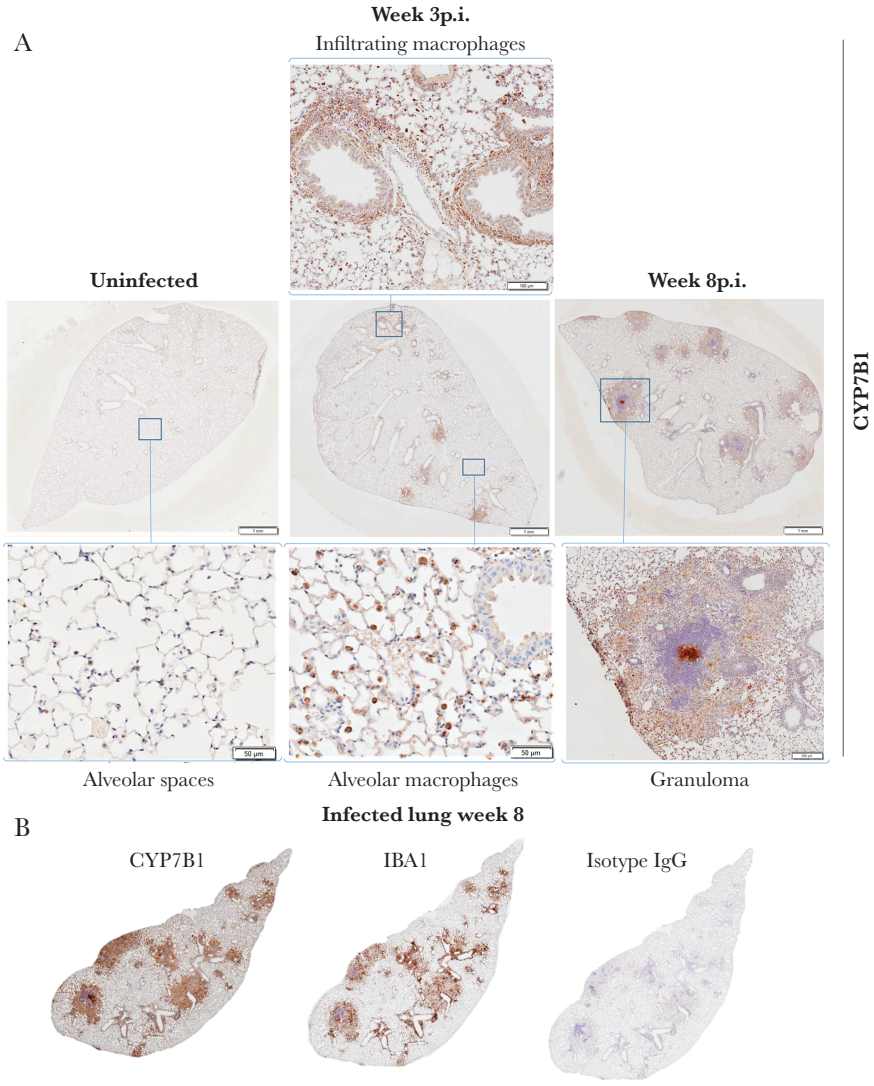

Figure 3. CYP7B1 protein expression in alveolar macrophages and in the center of tuberculosis granulomas. (A) Representative images of CYP7B1 immunolabeling on lung sections from uninfected and *Mycobacterium tuberculosis* (Mtb)-infected animals at 3 and 8 weeks postinfection. (B) Representative image of IBA1 immunolabled serial sections from the lungs of mice 8 weeks postinfection.

mice [27]. A delayed innate immune activation results in delayed adaptive immune priming. Consistent with this, GPR183KO mice had significantly lower IFN-β, IFN-γ, and a trend toward lower IL-1β production compared with WT controls [27]. We showed that during the later stages of infection, GPR183KO mice accumulated significantly more macrophages in the lung compared with WT animals through GPR183-independent mechanisms. These GPR183-independent mechanisms could include multiple other cellular targets of oxysterols involved in immune regulation [34] or could be chemokine mediated.

We found that a lack of GPR183 impacts mainly macrophage infiltration, even though this receptor is also expressed on other immune subsets. Consistent with our finding, others demonstrated that T cells do not require GPR183 for migration into the Mtb-infected lung [35]. We showed that CYP7B1 is almost exclusively expressed in alveolar macrophages and infiltrating macrophages upon Mtb infection and barely expressed in uninfected lungs. Thus, we identified macrophages as the major source of oxysterols in the Mtb-infected lung. Previous studies have reported high expression of CH25H by macrophages [13, 36–38], and we found that both CH25H and CYP7B1 are upregulated upon Mtb infection in both primary human monocytes and in THP-1 macrophages (data not shown), which is likely mediated by interferons because CH25H is interferon inducible [29]. In a cigarette smoke-exposed mouse model, Jia et al [25] demonstrated high expression of *Ch25h* in the airway epithelial cells, whereas Madenspacher et al [39] found that *Ch25h* and its product 25-OHC are highly expressed in resident lung alveolar macrophages, but not in macrophages from other compartments in LPS-exposed C57BL/6 mice. In lymphoid tissues,

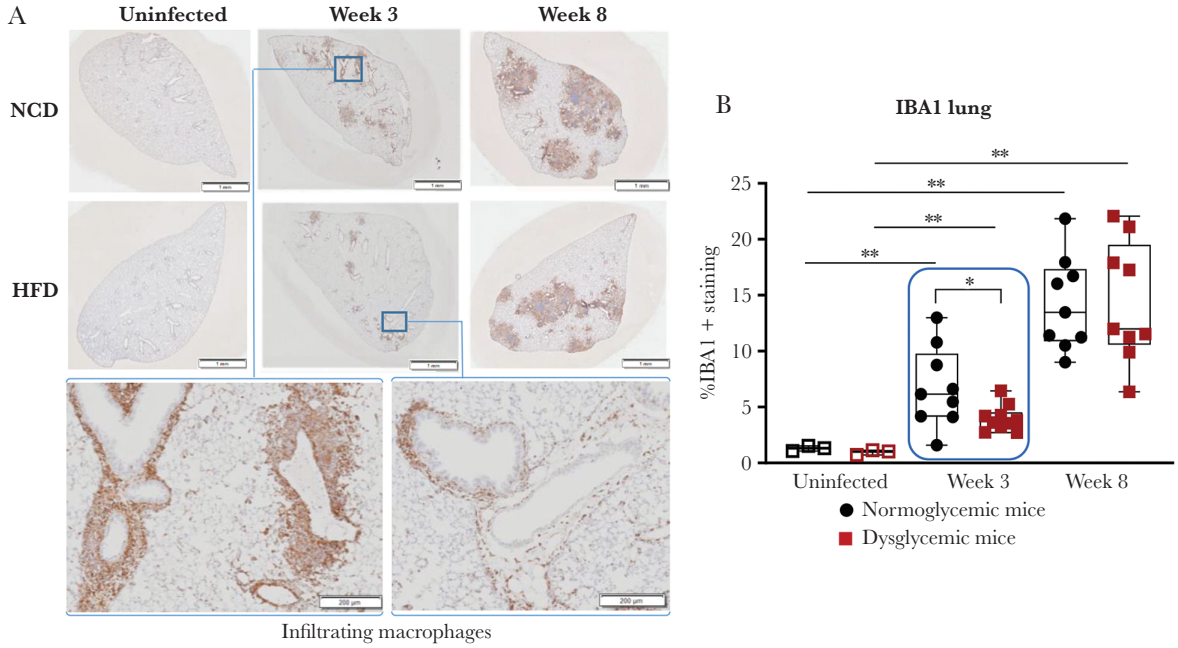

Figure 4. Reduced infiltration of macrophages in mice with dysglycemia at 3 weeks postinfection. (A) Representative images of the macrophage marker IBA1 immunolabeled lung sections from uninfected and *Mycobacterium tuberculosis* (Mtb)-infected animals at 3 and 8 weeks postinfection. (B) Quantitative analysis of IBA1(+) labeled areas as percentage of total lung section area. Data are means ± standard error of the mean of n = 9–10 mice from infected groups analyzed from 1 experiment. Circles represent normoglycemic mice and squares represent dysglycemic mice. Data analysis was performed by Mann-Whitney *U* test. *, $P < .05$; **, $P < .01$.

stromal cells have been reported to be the main *Ch25h* and *Cyp7b1* expressing cells and major contributors to 7α,25-OHC generation [31]. These data suggest that the cellular source of 7α,25-OHC-producing enzymes varies depending on the type of stimulus and local environment of the involved organs.

At the later time point 8 weeks postinfection, CYP7B1 was abundantly expressed in the center of granulomas compared with surrounding regions. This suggests that 7α,25-OHC is highly produced at the center of granulomas to attract other macrophages and lymphocytes making the oxysterol/GPR183 an important element in positioning immune cells in the granuloma. Another interesting observation in our study is that the intensity of CYP7B1 signals is not uniform throughout all granulomas from the same lung lobe and likely reflects

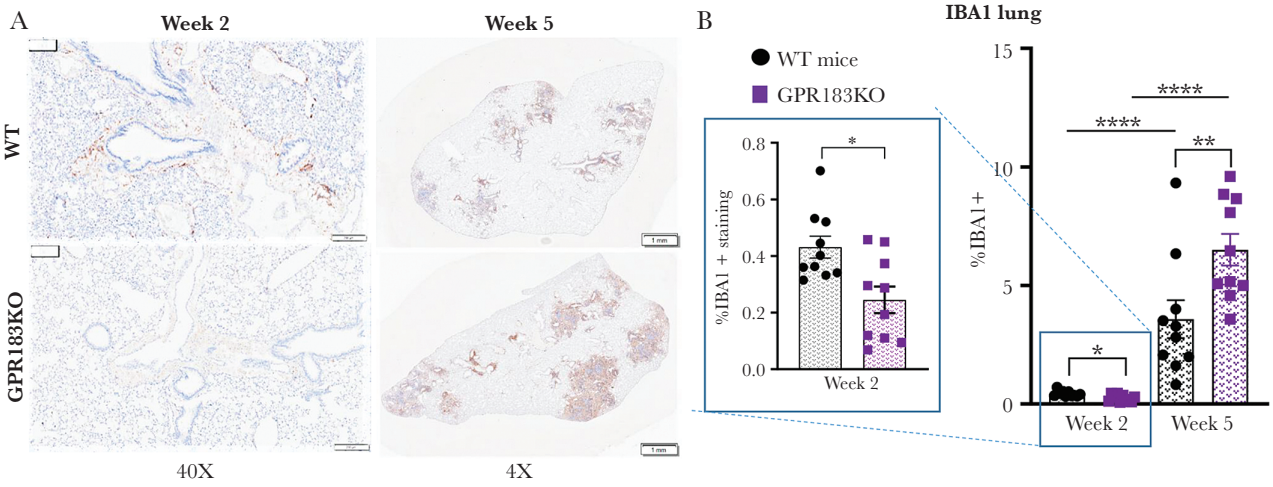

Figure 5. Reduced macrophage infiltration into the lung of GPR183KO mice at 2 weeks postinfection. Wild-type (WT) and GPR183KO mice were infected with *Mycobacterium tuberculosis* (Mtb) as previously described [27]. (A) Representative IBA1 immunolabeled lung sections from Mtb-infected WT and GPR183KO mice at 2 and 5 weeks postinfection (B). Quantitative analysis of IBA1-immunolabeled areas as percentage of total lung section area. Data are mean ± standard error of the mean of n =10 infected mice/group analyzed from 1 experiment. Circles represent C57BL/6 WT mice and squares represent GPR183KO mice. Data analysis was performed by Mann-Whitney *U* test. *, $P < .05$; **, $P < .01$; ****, $P < .0001$.

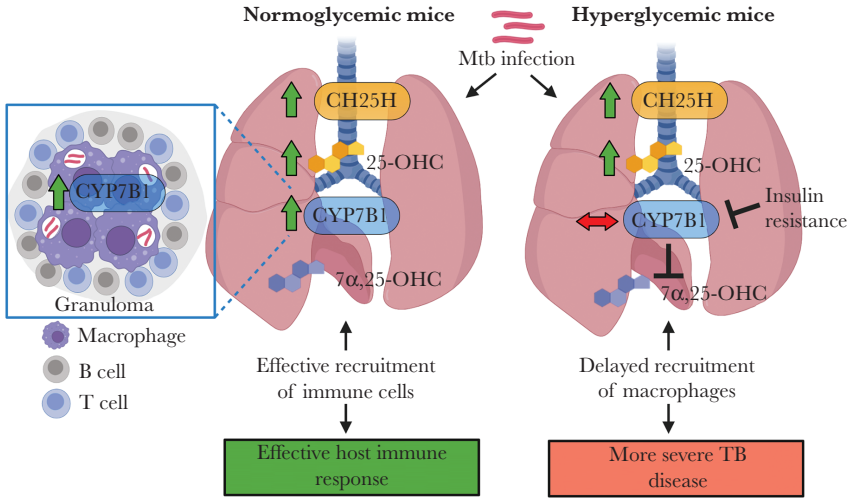

Figure 6. Schematic summary of the role of the oxysterols 25-OHC and 7α,25-OHC and GPR183 in *Mycobacterium tuberculosis* (Mtb)-infected normoglycemic and hyperglycemic mice. The enzymes Cholesterol 25-hydroxylase (CH25H) and Cytochrome P450 Family Subfamily B Member 1 (CYP7B1) are upregulated in the lung upon Mtb infection, resulting in increased production of the oxysterols 25-OHC and 7α,25-OHC, which in turn leads to effective recruitment of GPR183-expressing immune cells to the site of infection. CYP7B1 is predominantly expressed by macrophages in the center of tuberculosis (TB) granuloma surrounded by lymphocytes, and therefore the oxysterol/GPR183 axis may contribute to positioning these immune cells in TB granulomas. In high-fat diet fed hyperglycemic mice, this pathway is altered, with CYP7B1 mRNA and protein expression blunted, which leads to delayed recruitment of macrophages to the lung. (This figure was created with BioRender.).

heterogeneity of developmental stages of granulomas in the Mtb-infected lung [40–42].

The concentrations of oxysterols in serum are modified by diabetes and obesity with some up- and some downregulated [43, 44]. Aberrant oxysterol metabolism in diabetes is also present in the liver [45]. In an insulin-resistant, HFD-based mouse model, chronic suppression of CYP7B1 was observed in the liver accompanied by reduced production of 25-OHC [30]. However, whether oxysterol concentrations vary in the lung upon HFD feeding or diabetes has not been investigated. In this study, we demonstrate the Mtb-induced upregulation of CYP7B1 is blunted during dysglycemia. Reduced CYP7B1 expression likely results in reduced 7α,25-OHC production. A limitation of our study was that we were unable to measure this oxysterol due to technical constraints. However, a reduced 7α,25-OHC production in dysglycemic compared with normoglycemic mice can explain the delayed recruitment of macrophages to the site of infection. Delayed infiltration of myeloid cells to the Mtb-infected lung in diabetic mice has also been shown by others [6], which the authors attributed to aberrant chemokine production at a time when the significance of oxysterols in immune cell migration was not yet considered.

CONCLUSIONS

In summary, we have shown that Mtb infection results in increased expression of the oxysterol-producing enzymes CH25H and CYP7B1, increased production of 25-OHC, and likely also 7α,25-OHC in the lung (Figure 6). Expression of CYP7B1 is blunted in dysglycemic animals likely due to insulin resistance and associated with reduced macrophage infiltration during early infection, which is also observed in GPR183KO mice. We therefore demonstrated that the oxysterol/GPR183 axis is important for immune cell positioning and possibly granuloma formation in TB. Further studies are required to assess how administration of oxysterols or GPR183 ligands modifies TB pathogenesis and outcomes and whether such compounds can be exploited for host-directed therapies.

Supplementary Data

Supplementary materials are available at *The Journal of Infectious Diseases* online. Supplementary materials consist of data provided by the author that are published to benefit the reader. The posted materials are not copyedited. The contents of all supplementary data are the sole responsibility of the authors. Questions or messages regarding errors should be addressed to the author.

Notes

Acknowledgments. We acknowledge the Translational Research Institute for providing core facilities that enabled this research, particularly staff from the Biological Resources Facility and the Microscopy Facility.

Financial support. This work was funded by grants to K. R. from the National Institutes of Health, National Institute of Allergy and Infectious Diseases Grant Number R01AI116039, the Mater Foundation, the Australian Respiratory Council, and the Australian Infectious Diseases Research Centre. The Translational Research Institute is supported by a grant from the Australian Government.

Potential conflict of interests. M. M. R. is a cofounder of Antag Therapeutics and of Synklino. All authors have submitted the ICMJE Form for Disclosure of Potential Conflicts of Interest. Conflicts that the editors consider relevant to the content of the manuscript have been disclosed.

References

1. Critchley JA, Restrepo BI, Ronacher K, et al. Defining a research agenda to address the converging epidemics of tuberculosis and diabetes: part 1: epidemiology and clinical management. Chest **2017**; 152:165–73.
2. Sinha R, Ngo MD, Bartlett S, et al. Pre-diabetes increases tuberculosis disease severity, while high body fat without impaired glucose tolerance is protective. Front Cell Infect Microbiol **2021**; 11:691823.
3. Yamashiro S, Kawakami K, Uezu K, et al. Lower expression of Th1-related cytokines and inducible nitric oxide synthase in mice with streptozotocin-induced diabetes mellitus infected with Mycobacterium tuberculosis. Clin Exp Immunol **2005**; 139:57–64.
4. Martens GW, Arikan MC, Lee J, Ren F, Greiner D, Kornfeld H. Tuberculosis susceptibility of diabetic mice. Am J Respir Cell Mol Biol **2007**; 37:518–24.
5. Sugawara I, Yamada H, Mizuno S. Pulmonary tuberculosis in spontaneously diabetic goto kakizaki rats. Tohoku J Exp Med **2004**; 204:135–45.
6. Vallerskog T, Martens GW, Kornfeld H. Diabetic mice display a delayed adaptive immune response to Mycobacterium tuberculosis. J Immunol **2010**; 184:6275–82.
7. Podell BK, Ackart DF, Obregon-Henao A, et al. Increased severity of tuberculosis in Guinea pigs with type 2 diabetes: a model of diabetes-tuberculosis comorbidity. Am J Pathol **2014**; 184:1104–18.
8. Martinez N, Ketheesan N, West K, Vallerskog T, Kornfeld H. Impaired recognition of mycobacterium tuberculosis by alveolar macrophages from diabetic mice. J Infect Dis **2016**; 214:1629–37.
9. Mayer-Barber KD, Barber DL. Innate and adaptive cellular immune responses to mycobacterium tuberculosis infection. Cold Spring Harb Perspect Med **2015**; 5:a018424.
10. Bohrer AC, Castro E, Hu Z, et al. Eosinophils are part of the granulocyte response in tuberculosis and promote host resistance in mice. J Exp Med **2021**; 218:e20210469.
11. Bah SY, Dickinson P, Forster T, Kampmann B, Ghazal P. Immune oxysterols: role in mycobacterial infection and inflammation. J Steroid Biochem Mol Biol **2017**; 169:152–63.
12. Mutemberezi V, Guillemot-Legris O, Muccioli GG. Oxysterols: from cholesterol metabolites to key mediators. Prog Lipid Res **2016**; 64:152–69.
13. Hannedouche S, Zhang J, Yi T, et al. Oxysterols direct immune cell migration via EBI2. Nature **2011**; 475:524–7.
14. Rosenkilde MM, Benned-Jensen T, Andersen H, et al. Molecular pharmacological phenotyping of EBI2. An orphan seven-transmembrane receptor with constitutive activity. J Biol Chem **2006**; 281:13199–208.
15. Preuss I, Ludwig MG, Baumgarten B, et al. Transcriptional regulation and functional characterization of the oxysterol/EBI2 system in primary human macrophages. Biochem Biophys Res Commun **2014**; 446:663–8.
16. Gatto D, Paus D, Basten A, Mackay CR, Brink R. Guidance of B cells by the orphan G protein-coupled receptor EBI2 shapes humoral immune responses. Immunity **2009**; 31:259–69.
17. Pereira JP, Kelly LM, Xu Y, Cyster JG. EBI2 mediates B cell segregation between the outer and centre follicle. Nature **2009**; 460:1122–6.
18. Li J, Lu E, Yi T, Cyster JG. EBI2 augments Tfh cell fate by promoting interaction with IL-2-quenching dendritic cells. Nature **2016**; 533:110–4.
19. Suan D, Nguyen A, Moran I, et al. T follicular helper cells have distinct modes of migration and molecular signatures in naive and memory immune responses. Immunity **2015**; 42:704–18.
20. Gatto D, Wood K, Caminschi I, et al. The chemotactic receptor EBI2 regulates the homeostasis, localization and immunological function of splenic dendritic cells. Nat Immunol **2013**; 14:446–53.
21. Yi T, Cyster JG. EBI2-mediated bridging channel positioning supports splenic dendritic cell homeostasis and particulate antigen capture. Elife **2013**; 2:e00757.
22. Chu C, Moriyama S, Li Z, et al. Anti-microbial functions of group 3 innate lymphoid cells in gut-associated lymphoid tissues are regulated by g-protein-coupled receptor 183. Cell Rep **2018**; 23:3750–8.
23. Willinger T. Oxysterols in intestinal immunity and inflammation. J Intern Med **2019**; 285:367–80.
24. Shen ZJ, Hu J, Kashi VP, et al. Epstein-Barr virus-induced gene 2 mediates allergen-induced leukocyte migration into airways. Am J Respir Crit Care Med **2017**; 195:1576–85.
25. Jia J, Conlon TM, Sarker RS, et al. Cholesterol metabolism promotes B-cell positioning during immune pathogenesis of chronic obstructive pulmonary disease. EMBO Mol Med **2018**; 10:e8349.
26. Bottemanne P, Paquot A, Ameraoui H, Guillemot-Legris O, Alhouayek M, Muccioli GG. 25-Hydroxycholesterol metabolism is altered by lung inflammation, and its local administration modulates lung inflammation in mice. FASEB J **2021**; 35:e21514.
27. Bartlett S, Gemiarto AT, Ngo MD, et al. GPR183 regulates interferons, autophagy, and bacterial growth during mycobacterium tuberculosis infection and is associated with TB disease severity. Front Immunol **2020**; 11:601534.

28. McDonald JG, Smith DD, Stiles AR, Russell DW. A comprehensive method for extraction and quantitative analysis of sterols and secosteroids from human plasma. J Lipid Res **2012**; 53:1399–409.
29. Liu SY, Aliyari R, Chikere K, et al. Interferon-inducible cholesterol-25-hydroxylase broadly inhibits viral entry by production of 25-hydroxycholesterol. Immunity **2013**; 38:92–105.
30. Kakiyama G, Marques D, Martin R, et al. Insulin resistance dysregulates CYP7B1 leading to oxysterol accumulation: a pathway for NAFL to NASH transition. J Lipid Res **2020**; 61:1629–44.
31. Yi T, Wang X, Kelly LM, et al. Oxysterol gradient generation by lymphoid stromal cells guides activated B cell movement during humoral responses. Immunity **2012**; 37:535–48.
32. Emgard J, Kammoun H, Garcia-Cassani B, et al. Oxysterol sensing through the receptor GPR183 promotes the lymphoid-tissue-inducing function of innate lymphoid cells and colonic inflammation. Immunity **2018**; 48:120–32.e8.
33. Dunlap MD, Prince OA, Rangel-Moreno J, et al. Formation of lung inducible bronchus associated lymphoid tissue is regulated by mycobacterium tuberculosis expressed determinants. Front Immunol **2020**; 11:1325.
34. Reinmuth L, Hsiao C-C, Hamann J, Rosenkilde M, Mackrill J. Multiple targets for oxysterols in their regulation of the immune system. Cells **2021**; 10:2078.
35. Hoft SG, Sallin MA, Kauffman KD, Sakai S, Ganusov VV, Barber DL. The rate of CD4 T cell entry into the lungs during mycobacterium tuberculosis infection is determined by partial and opposing effects of multiple chemokine receptors. Infect Immun **2019**; 87:e00841–18.
36. Bauman DR, Bitmansour AD, McDonald JG, Thompson BM, Liang G, Russell DW. 25-Hydroxycholesterol secreted by macrophages in response to Toll-like receptor activation suppresses immunoglobulin A production. Proc Natl Acad Sci U S A **2009**; 106:16764–9.
37. Park K, Scott AL. Cholesterol 25-hydroxylase production by dendritic cells and macrophages is regulated by type I interferons. J Leukoc Biol **2010**; 88:1081–7.
38. Liu C, Yang XV, Wu J, et al. Oxysterols direct B-cell migration through EBI2. Nature **2011**; 475:519–23.
39. Madenspacher JH, Morrell ED, Gowdy KM, et al. Cholesterol 25-hydroxylase promotes efferocytosis and resolution of lung inflammation. JCI Insight **2020**; 5:e137189.
40. Hoff DR, Ryan GJ, Driver ER, et al. Location of intra- and extracellular M. tuberculosis populations in lungs of mice and guinea pigs during disease progression and after drug treatment. PLoS One **2011**; 6:e17550.
41. Plumlee CR, Duffy FJ, Gern BH, et al. Ultra-low dose aerosol infection of mice with mycobacterium tuberculosis more closely models human tuberculosis. Cell Host Microbe **2021**; 29:68–82.e5.
42. Hunter RL. Tuberculosis as a three-act play: a new paradigm for the pathogenesis of pulmonary tuberculosis. Tuberculosis (Edinb) **2016**; 97:8–17.
43. Guillemot-Legris O, Mutemberezi V, Cani PD, Muccioli GG. Obesity is associated with changes in oxysterol metabolism and levels in mice liver, hypothalamus, adipose tissue and plasma. Sci Rep **2016**; 6:19694.
44. Tremblay-Franco M, Zerbinati C, Pacelli A, et al. Effect of obesity and metabolic syndrome on plasma oxysterols and fatty acids in human. Steroids **2015**; 99:287–92.
45. Fu S, Fan J, Blanco J, et al. Polysome profiling in liver identifies dynamic regulation of endoplasmic reticulum translatome by obesity and fasting. PLoS Genet **2012**; 8:e1002902.